Effect of different annealing temperatures on the performance of $CsPbBr_3$ films and their solar cells

FEI ZHAO[1,*], YANNAN ZHANG[1], YIXIN GUO[2,*]

[1]*School of Photoelectric Engineering, Changzhou Institute of Technology, Changzhou, Jiangsu, 213032, China*

[2]*Department of Physics, Shanghai Normal University, Shanghai 200233, China*

All-inorganic $CsPbBr_3$ perovskite solar cells have attracted widespread attention due to their excellent stability. However, the poor crystal quality and large optical bandgap of $CsPbBr_3$ perovskite films limit the efficiency improvement of solar cells. Here, $CsPbBr_3$ perovskite films and corresponding solar cells are prepared by solution method. The effect of different annealing temperature on the performance of $CsPbBr_3$ perovskite films and corresponding solar cells is studied. The results show that compared with $CsPbBr_3$ solar cells annealed at 200 ℃ and 300 ℃, $CsPbBr_3$ solar cells annealed at 250℃ have higher efficiency (1.74%). The reason behind the efficiency improvement for $CsPbBr_3$ device is that $CsPbBr_3$ films with 250℃ annealing temperatures have better crystallinity and smaller optical band gap (2.344eV).

(Received December 7, 2024; accepted October 14, 2025)

Keywords: $CsPbBr_3$ film, Solar cell, Crystallinity, Optical band gap

1. Introduction

Organic inorganic hybrid perovskite solar cells have attracted widespread research interest from researchers due to their high photoelectric conversion efficiency (PCE) and low manufacturing cost. At present, the efficiency of organic-inorganic hybrid perovskite solar cell has increased from 3.8% to 26.1% [1-3]. Although its efficiency has rapidly improved, its air and thermal stability are extremely poor. The main reason for the poor stability of organic-inorganic hybrid devices is that the perovskite absorption layer contains organic components. These organic compounds are highly susceptible to moisture and temperature, leading to a sharp decline in device stability. Consequently, it is necessary to use inorganic elements to replace the organic elements in the organic-inorganic hybrid perovskite absorption layer. Cesium-based all-inorganic perovskite absorption layers ($CsPbI_3$, $CsPbI_2Br$, $CsPbIBr_2$, $CsPbBr_3$) have received widespread attention due to their ability to enhance device stability [4-7]. Compared with $CsPbI_3$, $CsPbI_2Br$ and $CsPbIBr_2$ cells, $CsPbBr_3$ cells have better stability [8-10]. The reason behind the improved stability of $CsPbBr_3$ solar cell is the presence of high-quality $CsPbBr_3$ absorbing layer in the device [11-13]. Accordingly, it is very important to study the $CsPbBr_3$ layer.

At present, the preparation methods of $CsPbBr_3$ films mainly include solution method [14] and thermal evaporation method [15]. Although $CsPbBr_3$ films prepared by thermal evaporation method have good crystallinity, they require high vacuum conditions during the preparation process. This makes the preparation process complex and the preparation cost high. The $CsPbBr_3$ film deposited by solution method can also achieve good crystallinity, and the preparation process is completely carried out in air during the film preparation, resulting in simplified preparation process and reduced preparation cost. Based on the above results, the solution method is more suitable for preparing high-quality $CsPbBr_3$ absorption layers. In this work, $CsPbBr_3$ films and corresponding solar cells are prepared by solution method. The effect of annealing temperature on the performance of $CsPbBr_3$ perovskite films and corresponding solar cells is studied by using XPS, XRD, SEM, absorption spectra and J-V curves. Compared with $CsPbBr_3$ solar cells annealed at 200℃ and 300℃, $CsPbBr_3$ solar cell annealed at 250℃ has a higher efficiency (1.74%).

2. Experimental methods

2.1. Device preparation

The FTO glass substrate was cleaned. The specific preparation steps of $CsPbBr_3$ perovskite film are as follows. Firstly, 367mg $PbBr_2$ powder (99.999%) was completely dissolved in 1ml dimethylformamide (DMF, 99.8%) solvent, and then the solution was spin coated onto an FTO glass substrate to form a $PbBr_2$ film. The spin coating speed and spin coating time were set to 2000rpm and 30s, respectively. Afterwards, the $PbBr_2$ film was annealed at 90℃for 30 min. Next, 15mg CsBr powder (99.999%) was completely dissolved in 1ml anhydrous methanol (99.8%), and then the solution spin coated onto $PbBr_2$ film. The spin coating speed and spin coating time were adjusted to 2000rpm and 30s, respectively. Then, the substrate with CsBr was annealed at 150℃, 200℃, 250℃ and 300℃ for 5min, respectively. It is worth noting that this step needs to be repeated four times, and the annealing temperature is the same each time. In this way, $CsPbBr_3$ perovskite films with different annealing temperatures were prepared. Then, the carbon paste is scraped onto $CsPbBr_3$ film and annealed at 120℃for 15 min. Finally, the solar cell with FTO/$CsPbBr_3$/C structure was manufactured and the effective area of the device was 0.09cm^2.

2.2. Characterizations

X-ray photoelectron spectroscopy (XPS) can be employed to determine the valence states of the elements in $CsPbBr_3$ samples. The crystallinity of $CsPbBr_3$ samples can be obtained through X-ray diffraction (XRD). The surface morphology of $CsPbBr_3$ samples can be characterized using scanning electron microscopy (SEM). The absorption spectra of $CsPbBr_3$ samples can provide their absorption coefficient and optical bandgap energy. The photovoltaic parameters of $CsPbBr_3$ solar cells can be acquired through the current density-voltage (J-V) curves.

3. Results and discussions

3.1. XPS analysis

Fig. 1 presents the XPS survey spectrum of the $CsPbBr_3$ film annealed at 250℃. As can be seen from Fig. 1, the characteristic peaks for Br 3d, Pb 4f and Cs 3d are observed, indicating that we may have fabricated the $CsPbBr_3$ film [7].

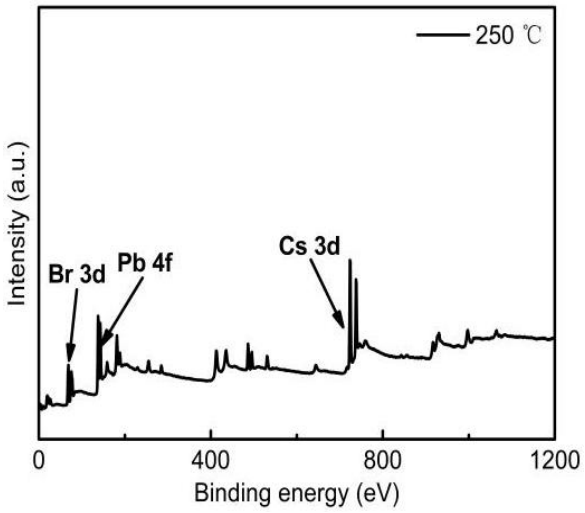

Fig. 1. XPS survey spectrum of the $CsPbBr_3$ film annealed at 250℃

3.2. XRD analysis

To further investigate the crystallinity of the sample, it is characterized by XRD. As shown in Fig. 2, two diffraction peaks for all samples appear at 21.51°and 30.72°. These two peaks correspond to the (110) and (200) crystal planes of the $CsPbBr_3$ perovskite film, respectively. This demonstrates that the $CsPbBr_3$ film has been successfully prepared. Additionally, a diffraction peak exists at 26.49°, which corresponds to the crystal plane of FTO. When the annealing temperature increases from 150℃ to 250℃, the intensities of the diffraction peaks corresponding to the (110) and (200) planes both increase, indicating higher crystallinity for the $CsPbBr_3$ film [16-18]. As the annealing temperature improves to 300℃, the intensities of their diffraction peaks decrease, showing a reduction in the crystallinity of the $CsPbBr_3$ film. The above phenomena suggest that an appropriate annealing temperature can enhance the crystallinity of the $CsPbBr_3$ film, but an excessively high annealing temperature can lead to a decrease in crystallinity. Therefore, the $CsPbBr_3$ film exhibits optimal crystallinity when the annealing temperature is 250℃.

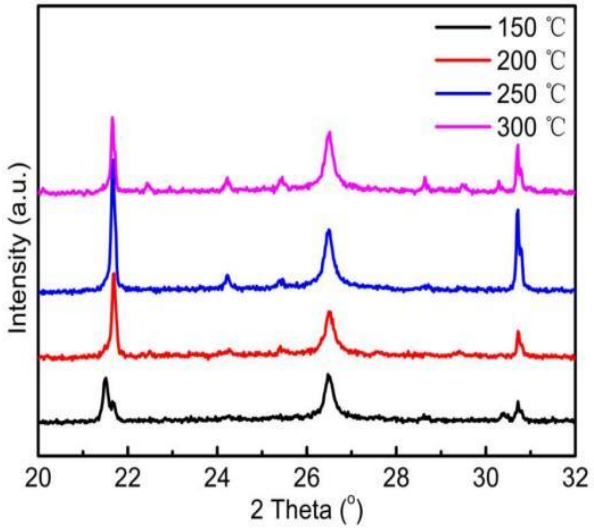

Fig. 2. XRD patterns of the $CsPbBr_3$ films annealed at different temperatures (colour online)

3.3. SEM analysis

Fig. 3a-3d present the SEM images of $CsPbBr_3$ perovskite films annealed at different temperatures. It can be observed from Fig. 3a-3d that the $CsPbBr_3$ perovskite film annealed at 150°C has three distinct holes, which shows poor crystallinity of the $CsPbBr_3$ film. When the annealing temperature increases to 250°C, the $CsPbBr_3$ film is free of holes and exhibits larger grains, suggesting improved crystallinity of the $CsPbBr_3$ film. Upon further increasing the annealing temperature to 300°C, a noticeable hole appears on the $CsPbBr_3$ film, indicating a decrease in crystallinity. Thus, the $CsPbBr_3$ film exhibits optimal crystallinity at an annealing temperature of 250°C, which is consistent with the XRD results. The crystallinity enhancement of the film is beneficial for the improvement of the open-circuit voltage (V_{oc}), short-circuit current density (J_{sc}) and fill factor (FF) of the solar cells.

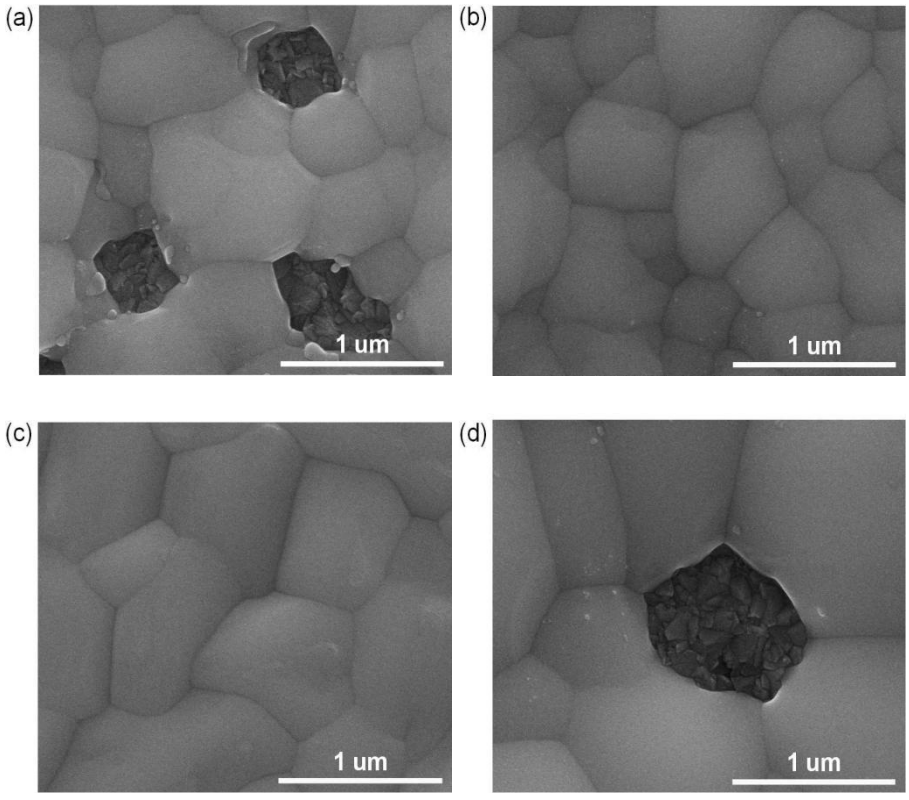

Fig. 3. SEM images of the $CsPbBr_3$ films annealed at (a) 150 ℃, (b) 200 ℃, (c) 250 ℃ and (d) 300 ℃

Fig. 4 shows the elemental mapping images of the $CsPbBr_3$ film annealed at 250°C. It can be observed from Fig. 4 that the distribution of each elemental ion within the $CsPbBr_3$ film annealed at 250°C is uniform, indicating that the prepared $CsPbBr_3$ film possesses good uniformity.

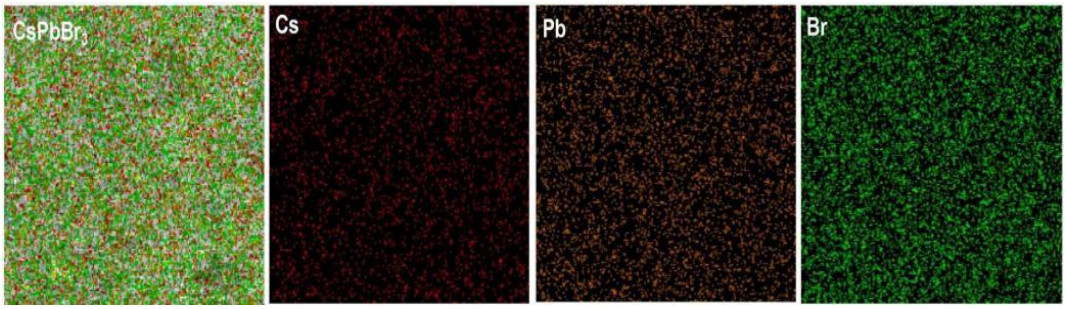

Fig. 4. Mapping diagram of the $CsPbBr_3$ film annealed at 250°C

3.4. Absorption spectra analysis

In addition to studying the microstructure of the sample, its optical properties also require further investigation. Fig. 5a shows the absorption spectra of $CsPbBr_3$ films annealed at different temperatures. As can be seen from Fig. 5a, the $CsPbBr_3$ film with 250°C annealing temperature exhibits higher absorptivity compared with the $CsPbBr_3$ film annealed at 200°C, which manifests that the $CsPbBr_3$ film can absorb more photons after annealing at 250°C [19,20]. As the annealing temperature increases to 300°C, the absorptivity of the $CsPbBr_3$ film decreases, suggesting that excessively high annealing temperatures can suppress the absorption of photons. The $CsPbBr_3$ film has the highest absorptivity at an annealing temperature of 250°C. The absorptivity for different samples is different. This phenomenon is due to the various crystallinity of different samples. Fig. 5b presents the curves of $(ahv)^2$ as a function of photon energy for different samples. The optical band gap (Eg) of the sample can be obtained from the curves of $(ahv)^2$ versus photon energy. The optical band gaps of the $CsPbBr_3$ films annealed at 200°C, 250°C, and 300°C are 2.354eV, 2.344eV and 2.356eV, respectively. For $CsPbBr_3$ films heated at different temperatures, the film heated at 250°C has a smaller optical band gap, implying that an appropriate annealing temperature can reduce the optical band gap of the film. The reduction of the optical band gap for the $CsPbBr_3$ film is beneficial for its absorption of more photons, leading to the increased J_{sc} of the device.

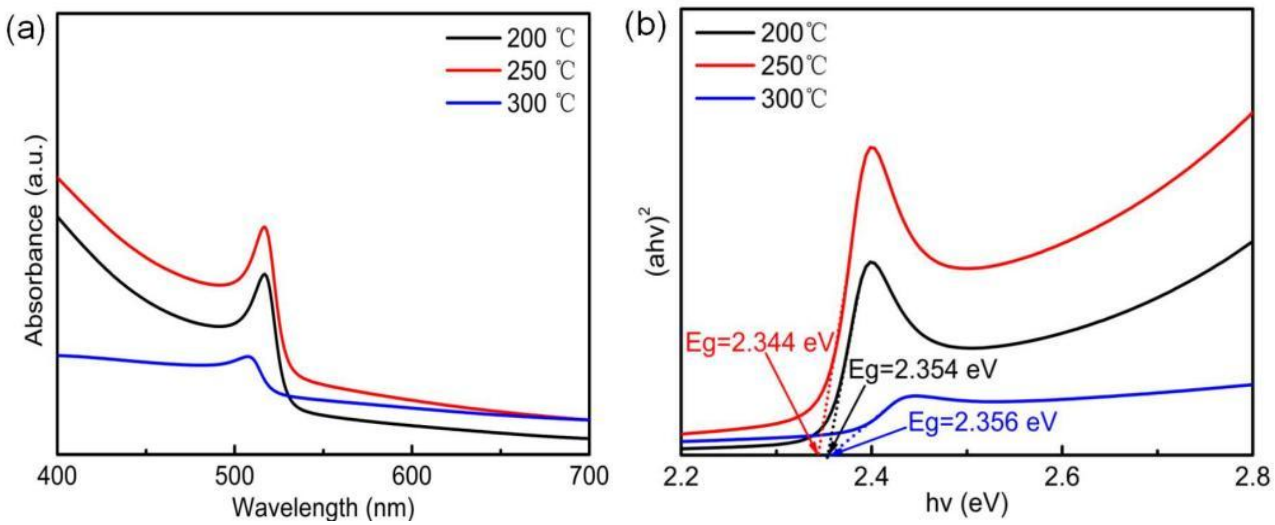

Fig. 5. (a) Absorption spectra of the $CsPbBr_3$ films annealed at different temperatures. (b) Curves of $(ahv)^2$ versus photon energy for different samples (colour online)

3.5. Device analysis

To investigate the photovoltaic performance of the $CsPbBr_3$ solar cells annealed at different temperatures, the J-V testing is conducted. The J-V curves of the $CsPbBr_3$ devices and their corresponding photovoltaic parameters are shown in Fig. 6 and Table 1, respectively. When the annealing temperature is 200°C, the $CsPbBr_3$ solar cell achieved a V_{oc} of 0.78V, a J_{sc} of 3.21mA/cm², a FF of 42.04% and a PCE of 1.05%. As the annealing temperature increases to 250°C, the V_{oc}, J_{sc}, FF and PCE of the $CsPbBr_3$ solar cell improved to 1.16V, 3.49mA/cm², 42.93% and 1.74%, respectively. The enhanced photovoltaic performance in the $CsPbBr_3$ device is attributed to the higher crystallinity, larger grain size and smaller optical band gap of the $CsPbBr_3$ film heated at 250°C. However, when the annealing temperature further increases to 300°C, the V_{oc}, J_{sc}, FF, and PCE of the device decrease to 0.91V, 2.54mA/cm², 32.97% and 0.76%, respectively. The reason for the decrease in the device performance is the deteriorated crystallinity and improved optical band gap of $CsPbBr_3$ films.

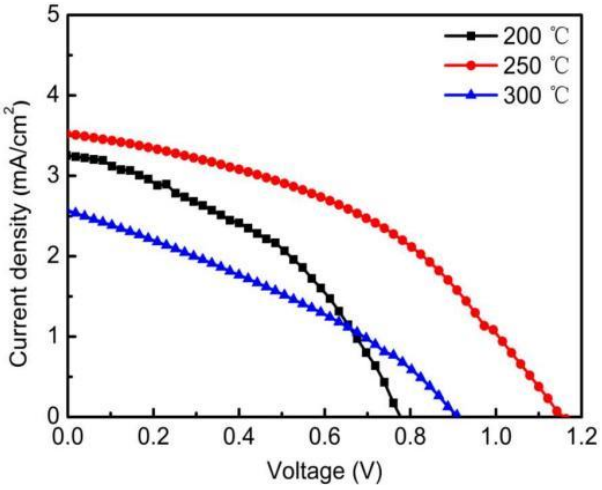

Fig. 6. J-V curves of the $CsPbBr_3$ solar cells annealed at different temperatures (colour online)

Table 1. Photovoltaic parameters of the $CsPbBr_3$ solar cells annealed at different temperatures

Annealing temperature (°C)	V_{oc} (V)	J_{sc} (mA/cm²)	FF (%)	PCE (%)
200	0.78	3.21	42.04	1.05
250	1.16	3.49	42.93	1.74
300	0.91	2.54	32.97	0.76

4. Conclusions

In this work, the $CsPbBr_3$ perovskite films are prepared by adjusting the annealing temperature. Through XRD, SEM and absorption spectroscopy tests, it is found that when the annealing temperature increases to 250°C, the $CsPbBr_3$ films have higher crystallinity, larger grain size and smaller optical band gap (2.344eV). As the annealing temperature further increases to 300°C, the crystallinity of the $CsPbBr_3$ film decreases and its optical band gap increases to 2.356eV. Hence, the $CsPbBr_3$ film with an annealing temperature of 250°C exhibits the highest crystallinity and the smallest optical band gap. Based on the above results, the $CsPbBr_3$ solar cells heated at 250°C are fabricated, achieving the best efficiency of 1.74%. This provides a novel pathway for the subsequent research of high-efficiency and stable $CsPbBr_3$ perovskite solar cells.

Acknowledgements

This work was financed by the Changzhou Scientific and Technological Program grant (Grant No. CJ20250087) and the National Natural Science Foundation of China (52402224, 12304043).

References

[1] A. Kojima, K. Teshima, Y. Shirai, T. Miyasaka, J. Am. Chem. Soc. **131**, 6050 (2009).
[2] J. Wang, Y. Qi, H. Zheng, R. Wang, S. Bai, Y. Liu, S. Hou, J. Mater. Chem. A **11**, 13201 (2023).
[3] J. Chen, Z. Wu, S. Chen, W. Zhao, Y. Zhang, W. Ye, J. Chen, Mat. Sci. Semicon. Proc. **174**, 108186 (2024).
[4] H. Dong, Z. Wang, Q. Zhang, Z. Zhang, Z. Zhu, X. Han, Z. Zou, Appl. Phys. Lett. **124**, 173903 (2024).

[5] Y. Guo, F. Zhao, Z. Li, J. Tao, D. Zheng, J. Jiang, J. Chu, Org. Electron. **83**, 105731 (2020).
[6] X. Tan, X. Liu, Z. Liu, B. Sun, J. Li, Appl. Surf. Sci. **499**, 143990 (2020).
[7] Y. Guo, F. Zhao, J. Tao, J. Jiang, J. Zhang, J. Yang, J. Chu, ChemSusChem **12**, 983 (2019).
[8] X. Jiang, C. Geng, X. Yu, J. Pan, H. Zheng, C. Liang, Y. Peng, ACS Appl. Mater. Interfaces **16**, 19039 (2024).
[9] H. Yuan, Y. Zhao, J. Duan, B. He, Z. Jiao, Q. Tang, Electrochim. Acta **279**, 84 (2018).
[10] G. Liao, J. Duan, Y. Zhao, Q. Tang, Sol. Energy **171**, 279 (2018).
[11] J. Duan, Y. Zhao, X. Yang, Y. Wang, B. He, Q. Tang, Adv. Energy Mater. **8**, 1802346 (2018).
[12] H. Yuan, Y. Zhao, J. Duan, Y. Wang, X. Yang, Q. Tang, J. Mater. Chem. A **6**, 24324 (2018).
[13] H. Guo, Y. Pei, J. Zhang, C. Cai, K. Zhou, Y. Zhu, J. Mater. Chem. C **7**, 11234 (2019).
[14] J. Zhu, Y. Liu, B. He, W. Zhang, L. Cui, S. Wang, Q. Tang, Chem. Eng. J. **428**, 131950 (2022).
[15] H. Li, G. Tong, T. Chen, H. Zhu, G. Li, Y. Chang, Y. Jiang, J. Mater. Chem. A **6**, 14255 (2018).
[16] Y. Zhao, Y. Wang, J. Duan, X. Yang, Q. Tang, J. Mater. Chem. A **7**, 6877 (2019).
[17] F. Zhao, Y. Guo, J. Tao, Z. Li, J. Jiang, J. Chu, Appl. Optics **59**, 5481 (2020).
[18] Y. Li, J. Duan, H. Yuan, Y. Zhao, B. He, Q. Tang, Solar RRL **2**, 1800164 (2018).
[19] X. Liu, X. Tan, Z. Liu, H. Ye, B. Sun, T. Shi, G. Liao, Nano Energy **56**, 184 (2019).
[20] X. Li, B. He, Z. Gong, J. Zhu, W. Zhang, H. Chen, Q. Tang, Solar RRL **4**, 2000362 (2020).

*Corresponding authors: fzhaobs@126.com; yxguo@shnu.edu.cn